Supporting Information for

# Enabling Continuous Immune Cell Recirculation on a Microfluidic Array to Study Immunotherapeutic Interactions in Recapitulated Tumour Microenvironment

Chun-Wei Chi[†,‡], Yeh-Hsing Lao[‡,⊥], AH Rezwanuddin Ahmed[†], Siyu He[⊥], Taha Merghoub[‡], Kam W. Leong[⊥,^] and Sihong Wang*[,†]

[†] Department of Biomedical Engineering, CUNY- City College of New York, New York NY, 10031, USA
[‡] Department of Pharmaceutical Sciences, University at Buffalo, The State University of New York, Buffalo, NY 14214, USA
[⊥] Department of Biomedical Engineering, Columbia University, New York, NY 10027, USA
[^] Department of Systems Biology, Columbia University Medical Center, New York, NY 10032, USA
[‡] Weill Cornell Medical College, New York, NY 10065, USA
* Corresponding author (shwang@ccny.cuny.edu)

**This document includes:**

## Supplementary Figures

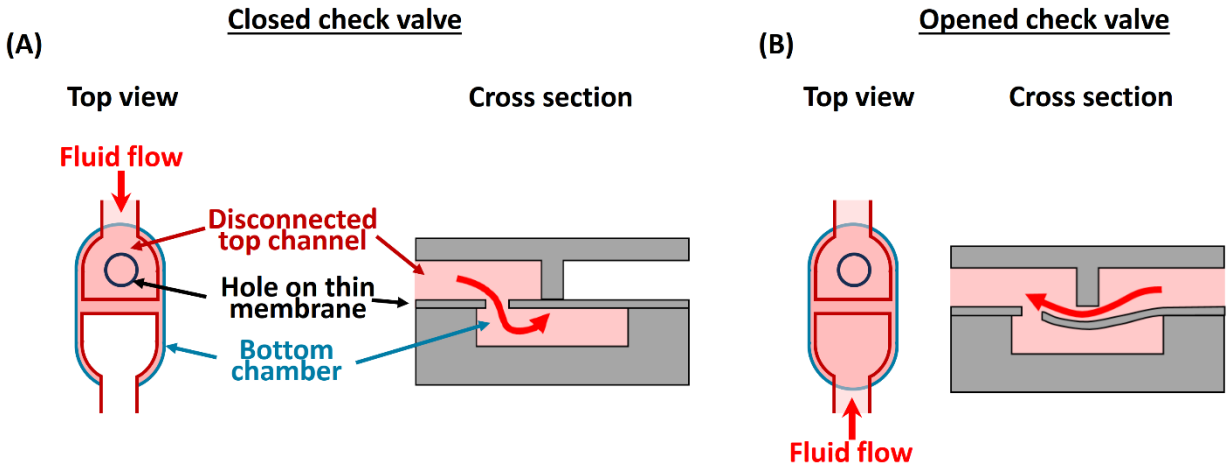


**Figure S1.** Design and working mechanism of our one-way check valves implemented in the recirculating circuit. In (A), the valve is closed because of the flow going from left to right; in (B) the valve is open because the flow going from right to left opens the junction between the stopper and the membrane.

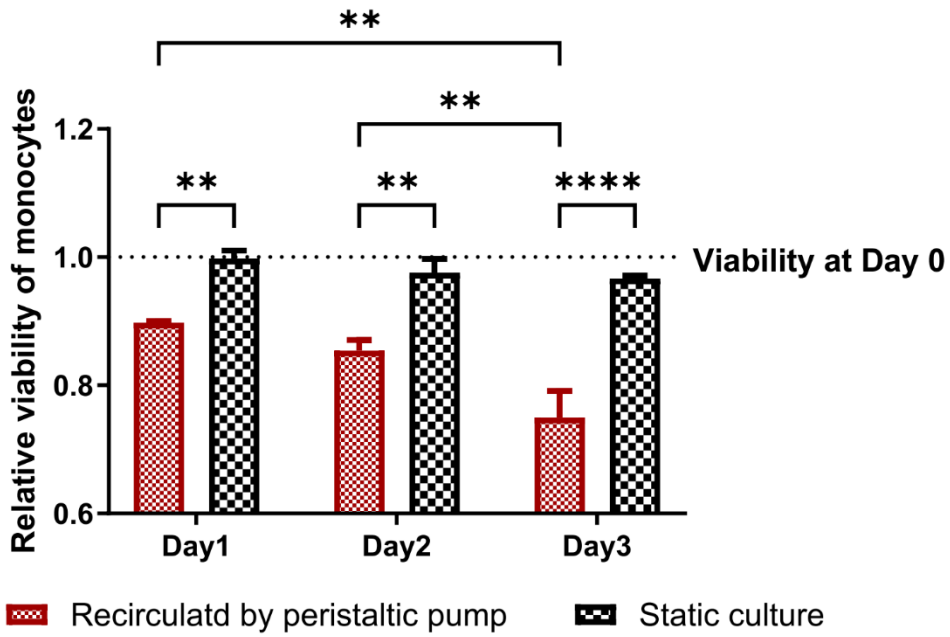


**Figure S2.** Cell viability of human monocyte line (THP-1) after continuously recirculating in a microfluidic channel using a micro-peristaltic pump (Bioptechs Delta T Micro-Perfusion Pump Ultra Low Flow). Results are presented as average ± standard deviation (S.D.; n = 3). Significance was determined using two-way ANOVA with Tukey Multiple Comparison Test and presented as **, $p < 0.01$ and ****, $p < 0.0001$.

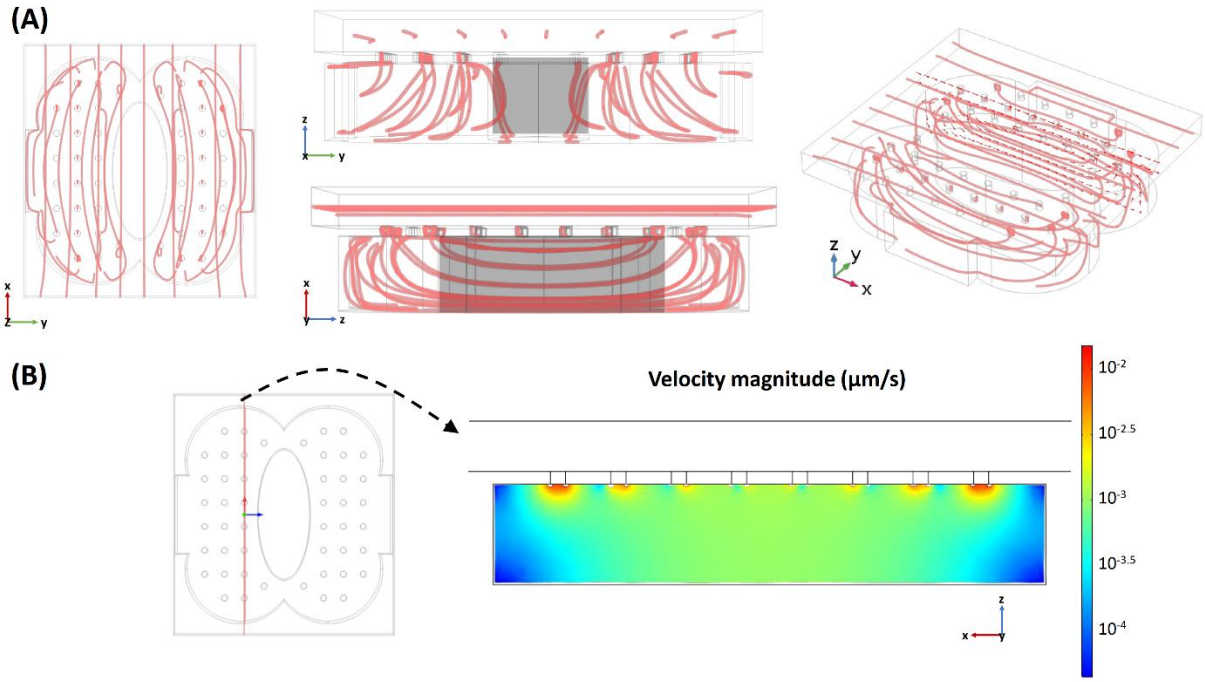


**Figure S3.** Results of fluid dynamics simulation in one unit of our 8x8 microfluidic cell array (μFCA). (A) Flow streamlines from top, side and 3D views. (B) 2D color gradient view of the velocity distribution in the bottom chamber along a selected plane using COMSOL.

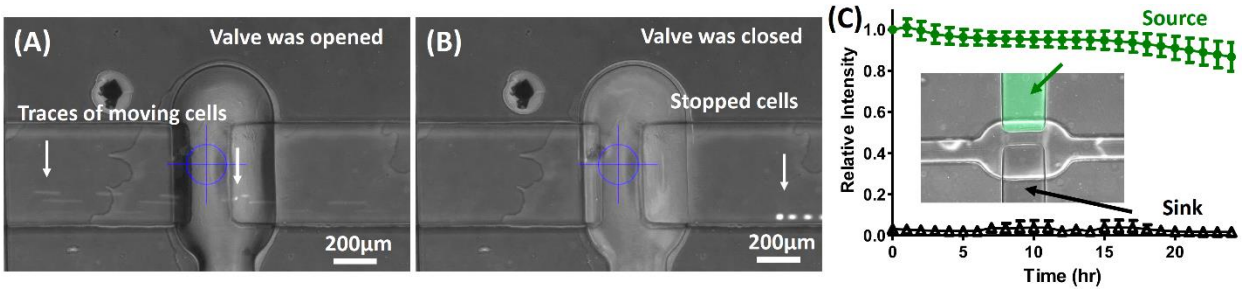


**Figure S4.** Representative images of pneumatic microvalve controlling the flow of fluorescence-labeled cells or solution to validate its leak-proof performance. (A) An image composite showing the traces of CellTracker-stained fibroblasts, captured in a 2-minute period when the microvalve was opened. Two representative trajectories of the cells are highlighted by arrows. (B) An image composite captured when the microvalve was closed. (C) Leakage test using sodium fluorescein. The sodium fluorescein dye was loaded to the source channel (top in the image), while deionized water was given in the sink channel (bottom). The microvalve was kept closed for 24 h, and the changes of fluorescence intensity in both channels were recorded over time to evaluate the leakage across the valve. Results are presented as average ± S.D. (n = 3).

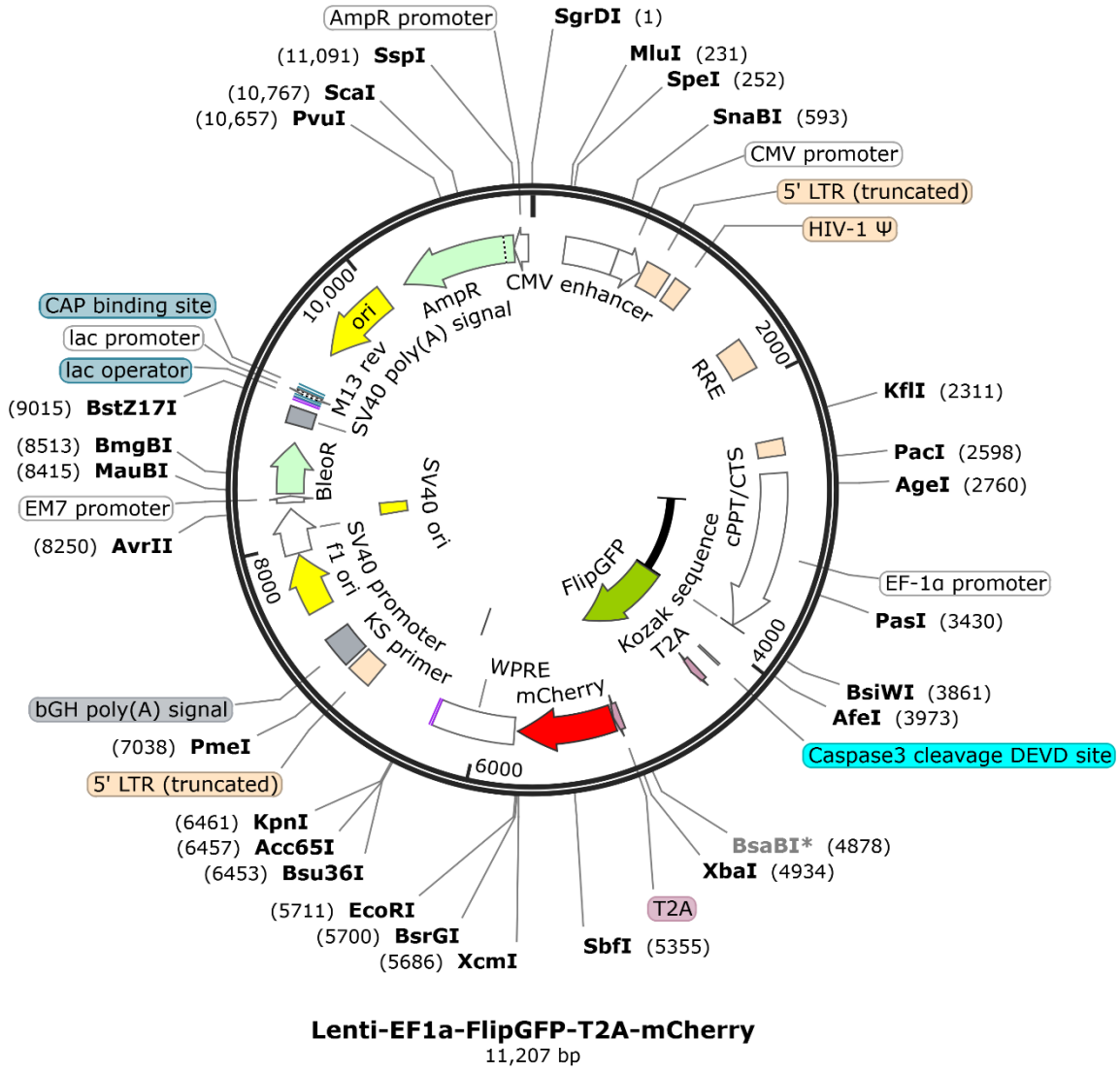


**Lenti-EF1a-FlipGFP-T2A-mCherry**
11,207 bp

**Figure S5.** Plasmid map of the lentiviral FlipGFP vector constructed in this study. Original FlipGFP-T2A-mCherry sequence was retrieved from the Addgene plasmid# 124428[1] and cloned into the other Addgene plasmid# 61422[2] by swapping the dCas9VP64-T2A-EGFP with FlipGFP.

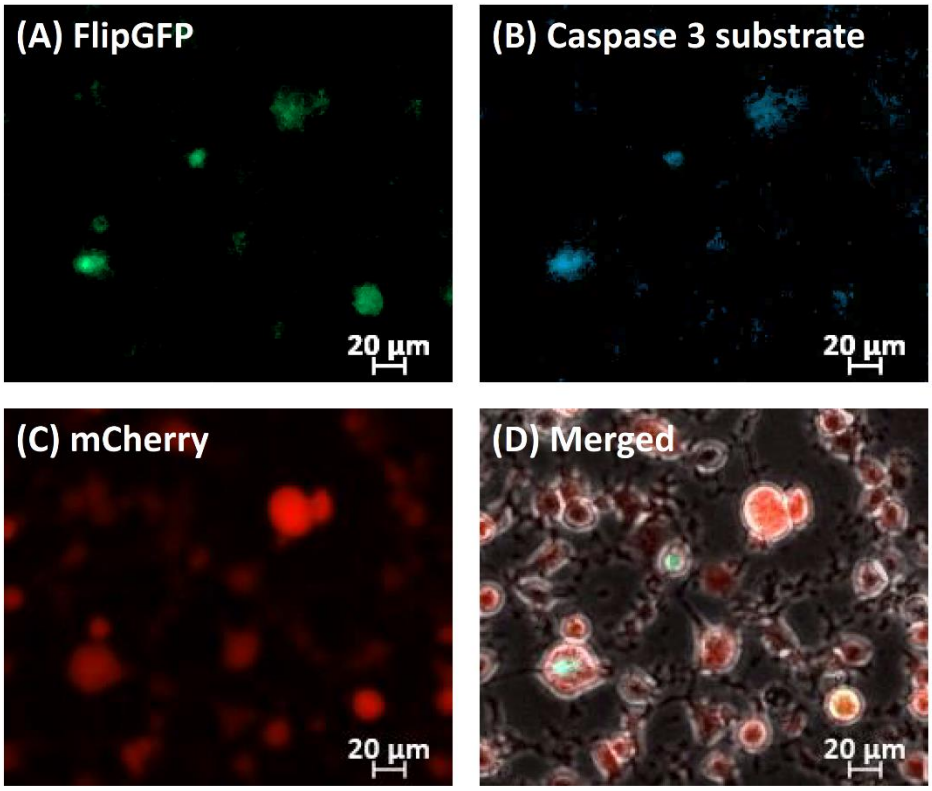


**Figure S6.** Response of FlipGFP-transduced MDA-MB-231 against apoptosis-inducing stimuli in triggering caspase 3 activity. After being treated with 1µM staurosporine for 5h, FlipGFP-transduced MDA-MB-231 cells showed (A) green fluorescence from the transduced FlipGFP and (B) blue fluorescence from an added caspase 3 substrate (NucView®405), each corresponding to the level of caspase 3 activity. (C) The constitutively expressed mCherry signals (red) confirm the successful transduction of FlipGFP-T2A-mCherry. (D) Merged image captured from phase contrast and all the fluorescent channels (FlipGFP, NucView®405 and mCherry) to confirm the overlap between FlipGFP and caspase 3 substrate signals.

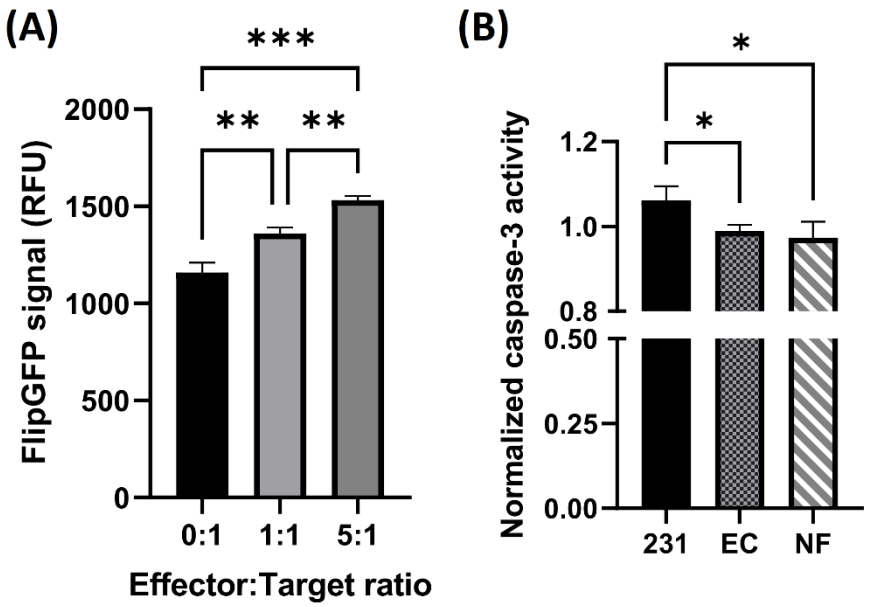


**Figure S7.** Cytotoxic effect of TALL-104 (Effector) against MDA-MB-231 (Target) and the stromal cells, endothelial cells (EC) and normal fibroblasts (NF). (A) FlipGFP signal quantification in the MDA-MB-231 cells incubated with TALL-104 under different effector: target (E:T) ratios for 3h. (B) TALL-104 cytotoxic effect on different cell types (cancer cells [231], endothelial cells [EC] or normal fibroblasts [NF]). Cells were incubated with TALL-104 in an E:T ratio of 2:1 for 2h and then stained with the caspase-3 substrate. Results are presented as average ± S.D. (n = 3). Significance was determined using one-way ANOVA with Tukey's Multiple Comparison Test and presented as *, $p < 0.05$; **, $p < 0.01$, ***, $p < 0.001$.

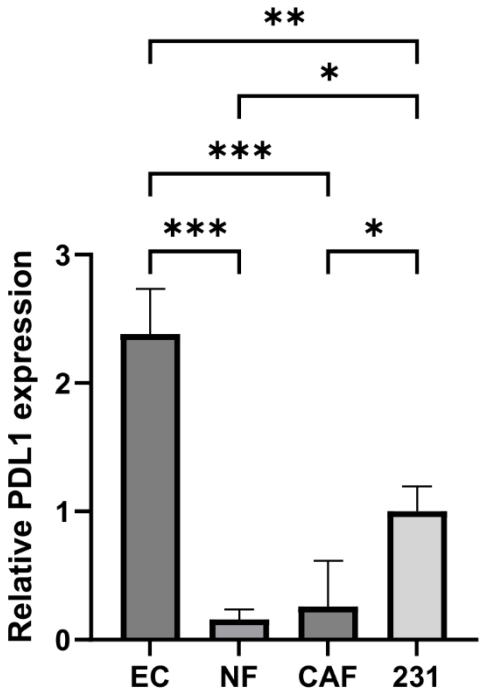


**Figure S8.** Relative PD-L1 mRNA expression level in each cell type measured by RT-qPCR. Results are presented as average ± S.D. (n = 3). Significance was determined using one-way ANOVA with Tukey's Multiple Comparison Test and presented as *, $p < 0.05$; **, $p < 0.01$, ***, $p < 0.001$.

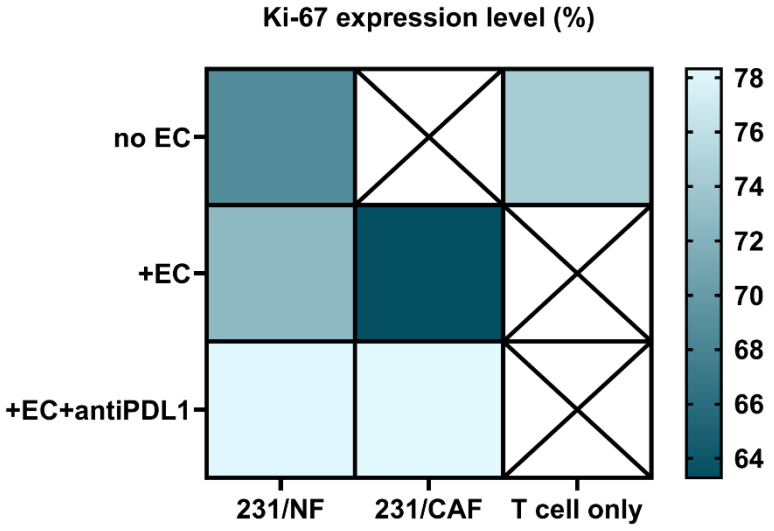


**Figure S9.** Relative Ki-67 expression of recirculated TALL-104 T cells collected from each culture condition at the end point. Results are presented as percentage of the number of Ki-67$^+$ cells over the total cell number. Ki-67 was measured by immunostaining. The crossed squares represent the conditions not tested in the experiment.

## Reference


1. Q. Zhang, A. Schepis, H. Huang, J. Yang, W. Ma, J. Torra, S. Q. Zhang, L. Yang, H. Wu, S. Nonell, Z. Dong, T. B. Kornberg, S. R. Coughlin and X. Shu, *J Am Chem Soc*, 2019, **141**, 4526-4530.
2. S. Konermann, M. D. Brigham, A. E. Trevino, J. Joung, O. O. Abudayyeh, C. Barcena, P. D. Hsu, N. Habib, J. S. Gootenberg, H. Nishimasu, O. Nureki and F. Zhang, *Nature*, 2015, **517**, 583-588.